Optical properties of amorphous films assembled from the nanoclusters of Ge - Al mixtures

1997 J. Phys.: Condens. Matter 9 10985

(http://iopscience.iop.org/0953-8984/9/49/016)

J. Phys.: Condens. Matter **9** (1997) 10985–10991. Printed in the UK PII: S0953-8984(97)85342-8

Optical properties of amorphous films assembled from the nanoclusters of Ge–Al mixtures

Bingyou Miao†, Jianmin Hong‡, Pingping Chen†, Xiaoli Yuan†, Min Han† and Guanghou Wang†§

† National Laboratory of Solid State Microstructures, Nanjing University, Nanjing 210093, People's Republic of China

‡ Modern Analysis Centre, Nanjing University, Nanjing 210093, People's Republic of China

Received 24 June 1997, in final form 15 September 1997

Abstract. Two samples of nanocluster-assembled Ge–Al thin films on quartz substrates have been fabricated by co-evaporation and inert-gas condensation. The thin films are amorphous and single phase, and the mean diameters of the nanoclusters are ∼8 nm and ∼45 nm, respectively. The composition of the nanoclusters in the two films is about 98.7 at.% Ge and 1.3 at.% Al, and the ratio of Ge and oxygen atoms is 1:1.8 (O). From the absorption spectra of the two samples, we estimate the optical gaps to be about 2.8 eV and 1.6 eV from Tauc plots, respectively; these are dependent on the nanocluster sizes and are much larger than those of vacuum-evaporated amorphous Ge and amorphous Ge–Al thin films. Under 3.32 eV (374 nm) excitation, photoluminescence (PL) peaks at 2.80 and 3.00 eV appear for the thin film with the mean diameter of the nanoclusters ∼8 nm; these can be interpreted as manifesting electron transitions from the optical gap (2.8 eV) and mobility gap (3.0 eV). In the absorption spectra of the two samples, a shoulder peak appears at 5.06 eV (245 nm), corresponding to the absorption band of one of the germanium oxygen-deficient centres (GODCs), namely GODC-1. The PL peak at 3.10 eV (400 nm), which arises from GODC-1, is also observed for the two samples.

Metal–semiconductor material systems have attracted great attention in recent years because of their technical applications. In general they can be divided into two groups: those forming intermetallic compounds such as Ge with Cu, Fe and Ni etc, and those which do not form thermodynamically stable compounds such as Ge with Al, Ga, Au and Ag etc.

From previous studies of $Ge_{1-x}Al_x$ thin films, we have obtained the following information. Ge-rich ($x < 0.3$) alloy film prepared by vacuum co-evaporation at room temperature [1–5] is amorphous and single phase. Al-rich alloy film ($0.4 < x < 0.9$) [6–8] shows aluminium crystals in an amorphous Ge–Al matrix. The density of segregated crystals decreases sharply as the germanium content is increased. The addition of Al results in a rapid and systematic decrease of the electric resistivity but increases the activation energy for Ge-rich amorphous films [9]. The temperature of the amorphous–crystalline transition decreases with the addition of Al for both Ge-rich and Al-rich thin films [8].

Some research has been concerned with the optical properties of vacuum-co-evaporated amorphous Ge–Al thin films. For Ge-rich films, the addition of a small (<2 at.%) amount of Al to Ge causes the absorption edge of amorphous Ge (a-Ge) to broaden and shift to higher energy, due to the reduction of the void concentration observed in a-Ge; but further

§ Author to whom any correspondence should be addressed.

0953-8984/97/4910985+07$19.50

increase of the Al concentration beyond 2 at.% causes the absorption to shift to lower energies and become more diffusive due to Al impurity states near the band edges, as in the case of crystalline Ge [10]. We have successfully prepared two amorphous Ge–Al thin films assembled from nanoclusters of different sizes by the co-evaporation method, and found that the optical gaps of the two films are dependent on the nanocluster sizes and are much larger than those of vacuum-evaporated a-Ge and amorphous Ge–Al thin films.

The thin films were fabricated by co-evaporation and the inert-gas condensation method [11]. The base pressure of the chamber was 7×10^{-6} Torr. A Ge–Al mixture of the powder composition (5 at.% Al) was firstly heated by melting high-purity (Ge: 99.999%; Al: 99.99%) powder constituents in a Mo boat for ten minutes in a vacuum of $\simeq 10^{-6}$ Torr. Ge–Al mixed films were co-deposited on quartz substrates at 293 K which were 72 mm above the Mo boat. The nanocluster size was controlled by adjusting the inert-gas pressure and evaporation temperature. The films were made in an Ar-gas atmosphere of 6.2×10^{-3} Torr (No 1) and 2.5×10^{-2} Torr (No 2) with an evaporation temperature of about 1200 °C. The film thicknesses estimated from the evaporation rates were about 150 nm (No 1) and 80 nm (No 2).

Quartz substrates were used for the optical absorption and photoluminescence (PL) measurements. The absorption spectra were taken using a U-3400 Spectrophotometer (190–2500 nm). The PL spectra were taken using a F-3010 Fluorescence Photospectrometer with correction for instrumental wavelength dependencies. The composition was obtained using a VF-3200 X-ray Spectrometer. For the transmission electron microscopy (TEM) study, Ge–Al mixed nanoclusters were directly deposited on a copper grid covered with a thin amorphous carbon film. The TEM studies were made by using a JEM-200CX operated at 200 kV. All of the characterizations were carried out at room temperature.

Figures 1(a) and 1(b) show TEM micrographs of samples No 1 and No 2. The inset in (a) is the selected-area diffraction (SAD) image of sample No 1, which is similar to that for sample No 2. It is clear that the films are amorphous and single phase (no Al or Ge crystals appear in the films according to the SAD image), and that nanocluster coalescence and superpositioning have occurred. The configuration of the nanocluster aggregation can be seen at the stage of fractal growth (most black spots correspond to island growth of the nanoclusters in three-dimensional space). From the non-aggregated nanoclusters in the TEM micrographs of the two samples, the nanocluster size can still be estimated. For sample No 1, the distribution of the nanoclusters is in the range 6–10 nm with a mean diameter of the nanoclusters of ∼8 nm. For sample No 2, the distribution of the nanoclusters is in the range of 40–50 nm with a mean diameter of the nanoclusters ∼45 nm.

The composition of the nanoclusters in the two films is about 98.7 at.% Ge and 1.3 at.% Al as obtained by x-ray spectrometry. The XPS data show that the binding energies of Ge 3d, Al 2p and O 1s electrons are 32, 80.6 and 531.9 eV, respectively. From the binding energies, we deduced that on the top surface of the two samples some of Ge atoms exist in the form of GeO_x (Ge 3d: ∼32.5 eV in GeO_2 and 29.0 eV in the Ge crystal [12]), but no Al atoms exist in the form of Al crystal (Al 2p: 72.89 eV) and Al_2O_3 (Al 2p: 75.72 eV) [13]. In this case, the Al atoms may be incorporated in an a-Ge matrix in one of the following ways: (1) they may be incorporated substitutionally in the Ge tetrahedra (true doping effects: a shallow acceptor level in Ge); (2) they may be accommodated by voids and dangling bonds [4, 9]. This means that Al atoms still exist in the a-Ge matrix as mentioned above when the films are assembled from the mixed Ge–Al nanoclusters. In addition, the ratio of Ge and O atoms is about 1:1.8 on the surface of the samples as indicated by XPS. The oxygen comes from two sources: (1) a very small number of oxygen atoms came from the evaporation process, since a little oxygen is still present at the chamber

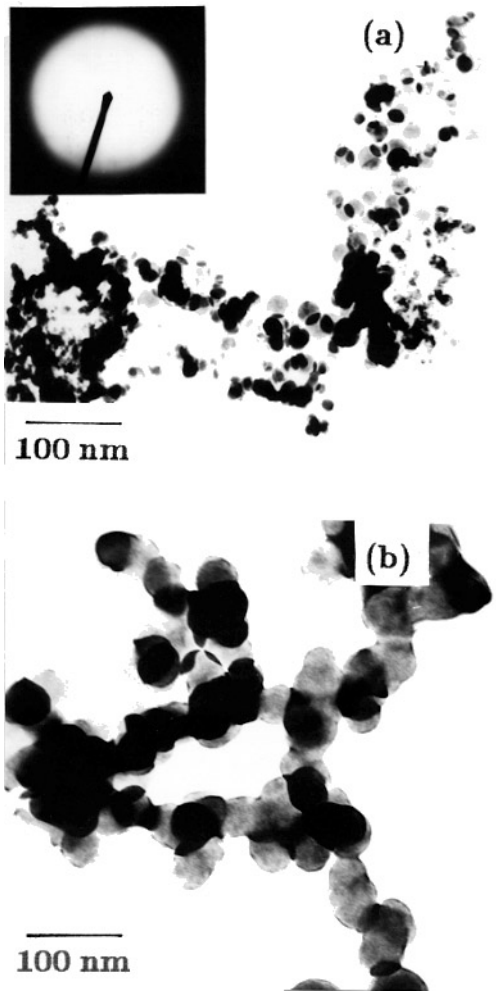

Figure 1. (a) and (b) are TEM micrographs of the samples No 1 and No 2, respectively. The inset in (a) is the SAD image for sample No 1, which is similar to that for sample No 2. The films are amorphous and single phase, and the mean diameters of the nanoclusters are ∼8 nm (No 1) and ∼45 nm (No 2) as indicated by TEM and SAD images. Nanocluster coalescence and superpositioning are apparent in the TEM micrographs.

pressure of 7×10^{-6} Torr; (2) most of the oxygen comes from the air. When the samples were taken out of the vacuum chamber, the surfaces were oxidized immediately in the air, as indicated by XPS.

Figure 2 shows the absorption spectra of the two films. In the energy range 3.26 eV to 5.17 eV the absorption increases sharply for sample No 1 but slowly for sample No 2. So do the optical absorption coefficients when the absorbance is corrected for the sample's thickness. It should be noted that there is no discrete absorption character in figure 2 (except the shoulder peak at around 5.06 eV (245 nm); we will discuss this later). According to the quantum confinement model, the Ge nanocrystals with mean diameters of 8 nm and 45 nm are in the strong- and medium-confinement regions (the Bohr radius of Ge is 24 nm) [14], and the lowest-confinement energies of electron–hole pairs in the single separated

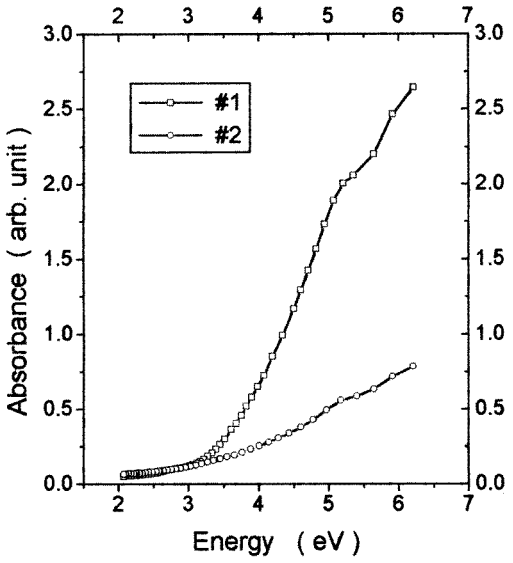

Figure 2. The absorption spectra of the two samples. A shoulder peak appears at 5.06 eV (245 nm) in the absorption spectra of the two samples. In the energy range 3.26 eV to 5.17 eV the absorption increases sharply for sample No 1 but slowly for sample No 2.

nanocrystals become discrete energy levels and vary with the nanocrystal size. So the discrete absorption character is expected to appear if the quantum confinement model for the Ge nanocrystals can be applied to the a-Ge nanoclusters. However, we have not observed a discrete absorption character for our two samples. Hence, the quantum confinement model for Ge nanocrystals may not be suitable for a-Ge nanoclusters.

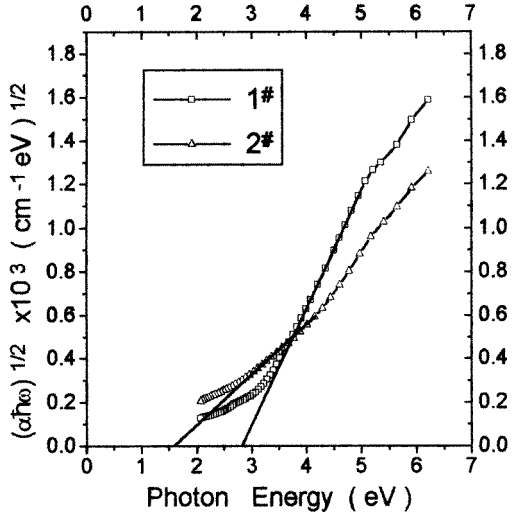

Figure 3. The Tauc plots for the two amorphous samples, whose optical gaps are about 2.8 eV (No 1) and 1.6 eV (No 2).

In order to contrast the optical gaps of the two samples assembled from different amorphous nanoclusters of Ge–Al mixtures (here the optical gap E_g^{opt} refers to the energy separating the localized states of the conduction and valence bands, or E_c and E_v, for a-Ge), we apply the commonly used $(\alpha\hbar\omega)^{1/2}$ versus $\hbar\omega$ relation ($\alpha \geqslant 10^4$ cm^{-1}) [15]:

$$\alpha\hbar\omega = c(\hbar\omega - E_g^{opt})^2$$

and easily get optical gaps of about 2.8 eV (No 1) and 1.6 eV (No 2), respectively. Figure 3

shows $(\alpha\hbar\omega)^{1/2}$ versus $\hbar\omega$ (Tauc's plots). It should be noted that the optical gaps of the two samples are much larger than that of vacuum-evaporated a-Ge or those of vacuum-co-evaporated amorphous Ge–Al thin films. For vacuum-evaporated a-Ge, the mobility gap (the energy separating the mobility edges (extended states) of the conduction and valence bands, or E_c^m and E_v^m for a-Ge) E_g^m is 0.88 eV at 300 K, but the optical gap E_g^{opt} is about 0.60 eV due to tail states [15]. For the vacuum-co-evaporated amorphous Ge–Al films, the largest optical gap is about 0.85 eV with 2 at.% Al concentration in the film [10].

From figure 3, we can see that the nanocluster size of the Ge–Al mixtures greatly influences the optical gap of the thin film assembled, for the same concentration of 1.3 at.% Al and oxygen ratio of 1 (Ge):1.8 (O) on the surface. A possible explanation is the following. As the a-Ge nanocluster size decreases, the Ge atomic ratio of the surface to the volume for the a-Ge nanocluster increases. The surface atoms of a-Ge nanoclusters, especially those prepared by evaporation, are loosely bonded and easily oxidized, so the electron motion in the core (the unoxidized part of a nanocluster) is confined by the interface ($Ge–GeO_x$) potential wall. The smaller the nanocluster, the stronger the confinement of the electron motion in the core of the a-Ge nanocluster. This confinement for electron motion in a-Ge nanoclusters may result in an enhancement of the optical gap of the thin film assembled.

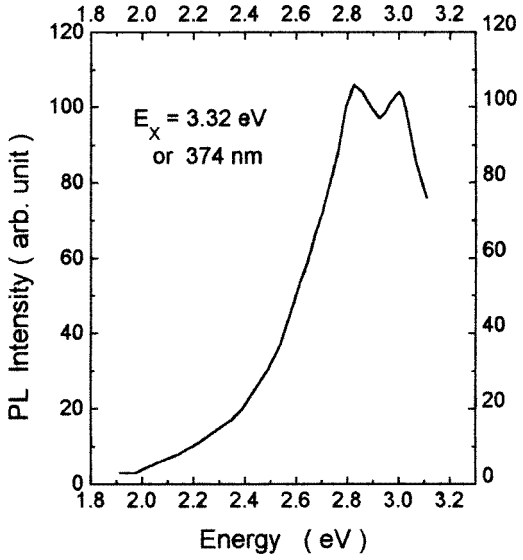

Figure 4. The PL spectrum of sample No 1 under 3.32 eV (374 nm) excitation. Two PL peaks, at 2.80 eV (443 nm) and 3.00 eV (413 nm), appear with a FWHM of ∼0.7 eV for the two PL peaks together.

Figure 4 shows the PL spectrum of sample No 1 under 374 nm excitation. There are two peaks, at 2.80 eV (443 nm) and 3.00 eV (413 nm) in the blue–purple region. The PL peak at 2.80 eV just corresponds to the optical gap of sample No 1 as shown in figure 3 and can be interpreted as manifesting electron transitions between localized states of conduction and valence bands. As reference [13] reported, Al atoms in a-Ge reduce the void concentration, and simultaneously form impurity states near the mobility edge E_v^m of the valence band (the shallow acceptor states). The localized states in the valence bands of the two samples mainly result from Al impurity states and void states. Therefore, the possibility of electron transitions between localized states increases due to the presence of Al impurity states. Another PL peak at 3.00 eV may correspond to the mobility gap of sample No 1, which can be interpreted as manifesting electron transitions between extended states of the conduction

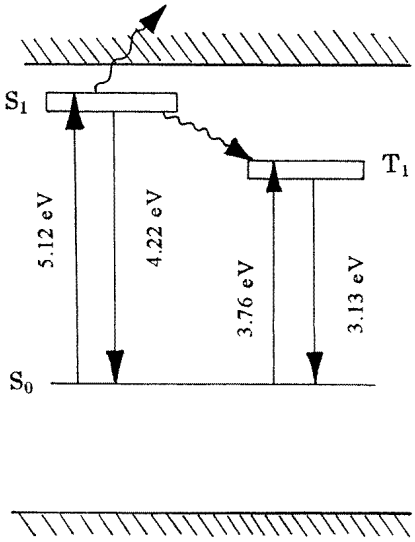

Figure 5. The energy level transitions of GODC-1 adopted from reference [17] (S and T represent the singlet and triplet). The shoulder peak at 5.06 eV (245 nm) in figure 2 can be ascribed to the $S_0 \longrightarrow S_1$ absorption band.

and valence bands. It is reasonable that the energy difference between the optical gap and the mobility gap is 0.2 eV for sample No 1. However, we are not able to observe the PL peak corresponding to the optical gap or the mobility gap from sample No 2, possibly due to the PL peak being too weak to be seen.

From figure 2, we can see that a shoulder peak appears at around 5.06 eV (245 nm) in the absorption spectra of the two samples. A similar absorption band at the same energy has been found in germanium-doped silica glass [16] and in germanosilicate glass and optical fibres (10 mol% GeO_2, 90 mol% SiO_2) [17]. Its intensity is dependent on the fusion temperature, the partial pressure of oxygen, and the quenching rate during the preparation process. The origin of the 5.06 eV absorption band can be ascribed to one of the germanium oxygen-deficient centres (GODCs), namely GODC-1 [17]. It is possible that Ge-related defect centres may exist in our two samples. The ratio of Ge and O atoms is about 1:1.8 on the surface of the two samples as indicated by XPS; voids and dangling bonds on the surfaces of the nanoclusters incorporate with oxygen atoms and then form Ge-related defect centres, such as the Ge E′ centre in which a Ge atom with an unpaired electron is bonded to three oxygens [16].

In figure 5 the energy levels of GODC-1, adapted from reference [17], are shown. According to the report in reference [17], the 5.06 eV (245 nm) band is attributable to the singlet–singlet transition $S_0 \longrightarrow S_1$, and the singlet–triplet transition $S_0 \longrightarrow T_1$ is partially forbidden. In comparison with the radiative transition, the $T_1 \longrightarrow S_0$ transition is excited efficiently, while the $S_1 \longrightarrow S_0$ transition is excited weakly or is not excited at all. For our two samples, we observed a PL peak at 3.10 eV (400 nm) as shown in figure 6, which is stronger for sample No 1, and can be attributed to the radiative transition $T_1 \longrightarrow S_0$ of GODC-1. The 4.77 eV (260 nm) excitation energy for the 3.10 eV PL peak is selected on the basis of the results given in reference [16]. For a pure quartz substrate, we did not observe any PL peak near 3.10 eV under 4.77 eV excitation. So we consider that the PL peak arises from the transition from a triplet to a singlet for GODC-1.

In summary, cluster-assembled Ge–Al nanofilms were prepared by co-evaporation and gas condensation. The cluster sizes are ∼8 nm and ∼45 nm and the films are amorphous and single phase, with compositions of 98.7 at.% Ge and 1.3 at.% Al. The optical gaps are

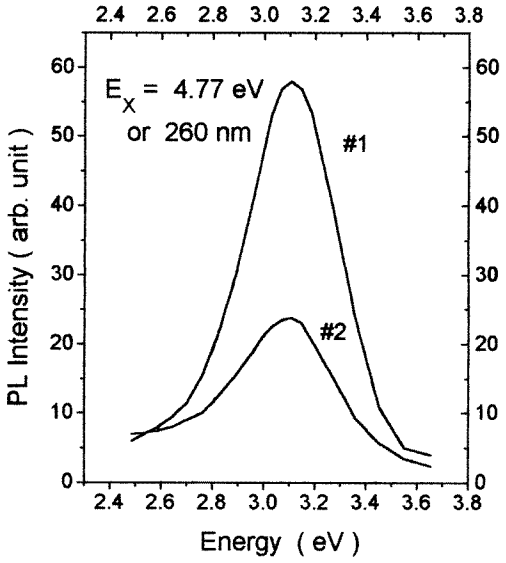

Figure 6. The PL peak at 3.10 eV (400 nm) for the two samples, which is stronger for sample No 1 and corresponds to the $T_1 \longrightarrow S_0$ transition of GODC-1 shown in figure 5.

estimated to be 2.8 eV for the former and 1.6 eV for the latter. The PL peaks are observed at 2.80 and 3.00 eV for the former, which can be explained as indicating an optical gap and a mobility gap. A shoulder in the absorption spectra can be identified at 5.06 eV, and a PL peak appears at 3.10 eV. Both may arise from GODC-1.

Acknowledgments

The authors gratefully acknowledge Yuying Fen and Zhong Li for making the absorption and PL measurements, and Drs Zaibing Guo, Fenqi Liu, and Minxiang Wang for assistance and discussions. This work was supported financially by the National Natural Science Foundation of China.

References

[1] Chopra K L, Nath P and Rastogi A C 1975 *Phys. Status Solidi* a **27** 645
[2] Randhawa H S, Malhotra L K and Chopra K L 1978 *J. Non-Cryst. Solids* **29** 311
[3] Chopra K L and Nath P 1976 *Phys. Status Solidi* a **33** 333
[4] Randhawa H S, Nath P, Malhotra L K and Chopra K L 1976 *Solid State Commun.* **20** 73
[5] Krapp M, Lambrecht A and Hasse J 1985 *Z. Phys.* B **61** 167
[6] Deutscher G, Rappaport M and Ovadyahu Z 1978 *Solid State Commun.* **28** 593
[7] Koster U 1972 *Acta Metall.* **20** 1361
[8] Catalina F and Afonso C N 1988 *Thin Solid Films* **176** 57
[9] Nath P, Dutta V and Chopra K L 1979 *J. Phys. C: Solid State Phys.* **12** L203
[10] Nath P, Pandya D K and Chopra K L 1976 *Phys. Status Solidi* a **34** 405
[11] Wang G H, Zhang H Q, Han M, Ma J X and Wang Q 1994 *Phys. Lett.* **189A** 218
[12] Maeda Y, Tsukamoto N, Yazawa Y, Kanemitsu Y and Masumoto Y 1991 *Appl. Phys. Lett.* **59** 3168
[13] Chen L and Hoffman R W 1993 *J. Vac. Sci. Technol.* A **11** 2303
[14] Yoffe A D 1993 *Adv. Phys.* **42** 173
[15] Tauc J, Grigorovici R and Vancu A 1966 *Phys. Status Solidi* **15** 627
[16] Gallagher M and Osterberg U 1993 *J. Appl. Phys.* **74** 2771
[17] Neustruev V B 1994 *J. Phys.: Condens. Matter* **6** 6901